fluids

MDPI

Article

Algebraic Prediction of Pressure and Lift for High-Angle-of-Attack Supersonic Asymmetric Delta Wings Based on Geometric Similarity

Xue-Ying Wang, Jie Peng and Zi-Niu Wu *

Department of Engineering Mechanics, Tsinghua University, Beijing 100084, China
* Correspondence: ziniuwu@mail.tsinghua.edu.cn

Abstract

In this paper, we explore the feasibility of deriving a simple, physically meaningful, and compact formulation for the pressure distribution and lift of an asymmetric delta wing at high angles of attack with an attached shock wave. Such a model would be valuable for rapid engineering analysis. Our approach begins with a compact pressure approximation in the linear regime, which is then extended to the nonlinear case through a geometric transformation and the assumption of functional similarity between linear and nonlinear solutions. This method bridges the solution in the central nonuniform flow region to the exact solutions in the uniform flow regions near the leading-edge shock waves, in a manner analogous to methods used for supersonic starting flow. The model is shown to reproduce existing results for both symmetric and yawed delta wings within an acceptable error margin, providing a compact explicit expression for the normal force coefficient as a weighted average of pressure coefficients from the two uniform flow regions. Additionally, we outline how the approach may be extended to the upper surface, where the uniform flow is described by swept Prandtl–Meyer relations.

Keywords: asymmetric delta wing; geometric similarity; pressure; lift; shock wave

1. Introduction

A linear solution for supersonic flow around delta wings was obtained in the 1940s and 1950s. For instance, Jones [1] based on slender-body assumptions, proposed a lift theory for low-aspect-ratio pointed wings, indicating that the spanwise loading distribution is elliptical and that lift varies little between subsonic and supersonic speeds. Stewart [2] employed conical flow theory and conformal mapping to solve the lift problem of delta wings at supersonic speeds, providing an analytical expression for the lift-curve slope and distinguishing between cases where the leading edge lies inside or outside the Mach cone. Puckett [3] used a source-distribution method to calculate the pressure coefficient of symmetric delta wings and obtained explicit formulas for the pressure coefficients in the two-dimensional and three-dimensional regions, and showed that the lift coefficient is equal to that of a two-dimensional wing, known from Ackeret [4]. Goodman [5] introduced a method for determining pressure distributions by canceling excess lift, applicable to both conical and non-conical flow regions, illustrated with examples such as rectangular wing tips and clipped delta wings. Malvestuto et al. [6], based on linearized supersonic flow theory, derived the lift and damping-in-roll derivatives for swept-back wings with streamwise tips and provided design curves.

Check for updates

Academic Editors: Zheng-Tong Xie and Olga A. Azarova

Received: 19 December 2025
Revised: 16 January 2026
Accepted: 21 January 2026
Published: 24 January 2026

Copyright: © 2026 by the authors. Licensee MDPI, Basel, Switzerland. This article is an open access article distributed under the terms and conditions of the Creative Commons Attribution (CC BY) license.

For the problem of supersonic/hypersonic flow with attached shock waves over the lower surface of delta wings, particularly under conditions of significant sweep angle and angle of attack where linear theory fails, several theoretical approaches have been developed. These methods crucially employ the exact oblique shock relations to define the uniform flow near the leading edges [7]. The central nonuniform flow region is then addressed using distinct methodologies: the thin shock-layer approximation, which leads to solutions constructed from discontinuous shock slopes [8,9]; the method of integral relations, which reduces the governing equations to ordinary differential equations [10]; and a unified perturbation theory that applies a linearized analysis on a nonlinear base flow and uses a strained coordinate technique for matching [11]. Hui [12] also extended the unified perturbation theory to yawed symmetric wings.

All these approaches fundamentally rely on the application of the shock relations to properly account for the three-dimensional, nonlinear effects of sweep and incidence. Roe [13] derived an exact expression for the spanwise pressure gradient at the boundary between the uniform and nonuniform flow regions beneath a supersonic delta wing with an attached shock. Fowell [14] considered both lower and upper surfaces of a delta wing, and his analysis revealed the existence of a critical angle of attack on the expansion surface, beyond which the flow becomes discontinuous, forming a shock structure. The flow past the upper surface of the wing was also investigated by Babaev [15]. Since Bluford [16], the effect of viscosity can be accounted for using numerical simulation. In the NASA technical paper by Wood [17], the aerodynamic characteristics of delta wings at lifting conditions were evaluated for the effects of wing leading-edge sweep, leading-edge bluntness, and wing thickness and camber, and then summarized in the form of graphs.

For the flow over delta wings at high angles of attack, the theoretical prediction of surface pressure under asymmetric conditions—whether induced by geometric dissimilarity between the left and right leading edges or by a yawed inflow—presents a significant challenge beyond the scope of classical linear theory. Early nonlinear analyses, such as the unified perturbation theory developed by Hui for yawed symmetric wings [12], provided a rigorous theoretical framework capable of handling the coupled effects of sweep and incidence across supersonic and hypersonic regimes. In his work, the asymmetry originates from the yaw angle of the oncoming stream, and the solution is constructed through a sophisticated perturbation approach combined with the method of strained coordinates to match the nonuniform central flow with the exact uniform flows near the leading edges. While theoretically comprehensive, such methods often result in solutions that are implicit or require considerable computational effort for evaluation, limiting their immediate utility for rapid engineering estimation.

Engineering applications usually require simpler, yet accurate and physically sound methods for predicting the lift and pressure distributions over asymmetric delta wings, particularly at high angles of attack.

Motivated by the need for a simpler yet physically sound predictive tool, this paper proposes a geometric transformation approach for asymmetric delta wings with dissimilar sweep angles and with supersonic upstream flow at a Mach number such that there are attached shock waves and there are two uniform two-dimensional flow regions enclosing a three-dimensional nonuniform flow region in the middle. The geometric transformation has been used by Bai & Wu [18] for extension of the linear solution of Heaslet & Lomax [19] to the nonlinear case in the application of supersonic starting flow at high angle of attack. The problem treated in this paper is different from Bai & Wu [18], so the geometric transformation has to be reformulated in a form suited to the problem.

The idea is to transform the linear solution, like that given by Puckett [3] (Equation (35)) for symmetric delta wings, of asymmetrical delta wings, originally expressed in terms of

the spanwise coordinate into a geometrically invariant form, and then replace the pressure coefficients pertinent to the two-dimensional uniform flow region by the attached shock solution. This way gives a very simple, physically relevant formula for both two-dimensional and three-dimensional regions over the asymmetrical delta wing.

The linear pressure expression for asymmetric delta wings is provided in Section 2. The nonlinear extension by geometric transformation is given in Section 3. Section 4 presents a comparison with exact solutions for both symmetric delta wings and asymmetric delta wings. Sections 3 and 4 treat the lower surface. Section 4 gives the expression for the normal force coefficient. Appendix A provides a possible method to extend the present result to the upper surface of an asymmetric delta wing.

2. Linear Solution for Asymmetric Delta Wing

2.1. Asymmetric Delta Wings Configuration

Consider an asymmetric delta wing with different sweep angles χ_1 (left) and χ_2 (right). The free stream Mach number is Ma_∞ and the angle of attack is α (assumed to be small in the linear case). See Figure 1 for a schematic display.

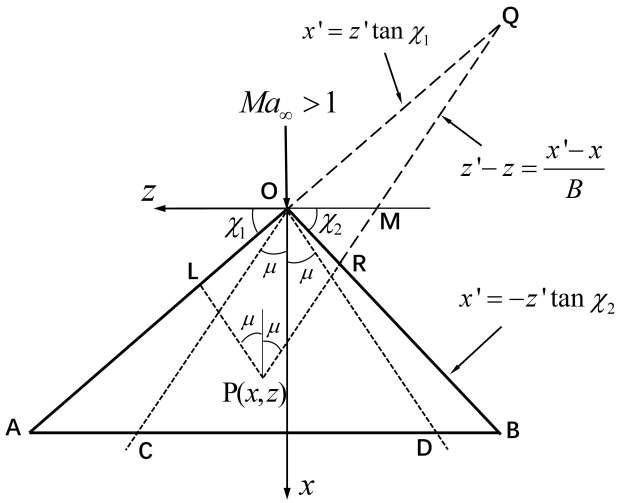


Figure 1. Schematic display of a delta wing. The coordinate system is defined with x along the chordwise direction, z along the spanwise direction, and y normal to the wing surface.

The two leading edges, OA and OB, are defined by

$$x = z\tan\chi_1 \text{ (left)}; \; x = -z\tan\chi_2 \text{ (right)}.$$

Supersonic leading edge conditions are assumed, so

$$Ma_\infty\cos\chi_1 > 1 \quad \text{and} \quad Ma_\infty\cos\chi_2 > 1$$

The Mach angle is $\mu_\infty = \arcsin\frac{1}{Ma_\infty}$. As usual, define $B = \sqrt{Ma_\infty^2 - 1}$, so $\tan\mu_\infty = \frac{1}{B}$. We also denote

$$m_1 = \frac{B}{\tan\chi_1} = \frac{1}{\tan\chi_1\tan\mu_\infty}, \quad m_2 = \frac{B}{\tan\chi_2} = \frac{1}{\tan\chi_2\tan\mu_\infty}.$$

For supersonic leading edges, we have $m_1 > 1$ and $m_2 > 1$.

The flow region is divided into a two-dimensional (2D) flow region near each leading edge, and a three-dimensional (3D) flow region (see Figure 1). The boundaries between

2D and 3D regions, OC and OD, are in fact the Mach waves or boundaries of the Mach cone, i.e.,

$$x = \frac{z}{\tan \mu_\infty} \text{ (left)}; \; x = -\frac{z}{\tan \mu_\infty} \text{ (right)}$$

2.2. Pressure Coefficient Expression

For the left 2D region ($z > 0$ and $x < Bz$), the pressure coefficient is given by Ackeret's [4] solution when the swept effect is accounted for

$$C_p = C_{p,1}^{(2d)} = \pm \frac{2\alpha m_1}{B\sqrt{m_1^2 - 1}}. \tag{1}$$

Similarly, for the right 2D region ($z < 0$ and $x < -Bz$), the pressure coefficient is given by

$$C_p = C_{p,2}^{(2d)} = \pm \frac{2\alpha m_2}{B\sqrt{m_2^2 - 1}}. \tag{2}$$

The flow in the three-dimensional (3D) flow region (inside the Mach cone from point O, i.e., $x > B|z|$) is conical, and the pressure coefficient is a function of

$$\eta = \frac{Bz}{x} \tag{3}$$

with $\eta = 1$ for left Mach wave (OC) and $\eta = -1$ for right Mach wave (OD).

We will see below that the pressure coefficient at point $P(x, z)$ in the three-dimensional region can be expressed as

$$C_p^{(3d)} = C_{p,1}^{(2d)} \Gamma_1(m_1, \eta) + C_{p,2}^{(2d)} \Gamma_2(m_2, \eta) \tag{4}$$

where $\Gamma_1(m_1, \eta)$ and $\Gamma_2(m_2, \eta)$ satisfy $\Gamma_1(m_1, 1) = \Gamma_2(m_2, -1) = 1$ and $\Gamma_1(m_1, -1) = \Gamma_2(m_2, 1) = 0$ to ensure that (4) reduces to the two-dimensional solutions at $\eta = \pm 1$.

The expressions for $\Gamma_1(m_1, \eta)$ and $\Gamma_2(m_2, \eta)$ can be obtained following the linear supersonic flow theory of Puckett [3]. At point $P(x, z)$ in the three-dimensional region as shown in Figure 1, $C_p(x, \pm 0, z)$ is given by

$$C_p(x, \pm 0, z) = \mp \frac{2\alpha}{\pi} \frac{\partial}{\partial x} \iint_{S_\Omega} \frac{dx'dz'}{\sqrt{(x - x')^2 - B^2(z - z')^2}}, \tag{5}$$

where S_Ω is the upstream region bounded by the Mach cone from P and the two wing leading edges.

The linear pressure expression (5) is solved using a technique proposed by Puckett [3]. This technique consists to decompose (5) into

$$C_p(x, \pm 0, z) = \pm \frac{2\alpha m_1}{B\sqrt{m_1^2 - 1}} \mp \frac{2\alpha}{\pi} \frac{\partial}{\partial x} \iint_{S_{OQR}} \frac{dx'dz'}{\sqrt{(x - x')^2 - B(z - z')^2}} \tag{6}$$

where the first term on the right-hand side is a two-dimensional flow solution and the second term (integral) is defined over the fictive triangle S_{OQR}, formed by points O, R, and Q, where Q is the intersection of the left leading edge and the extended line of PR (see Figure 1). The expression for $\frac{\partial I(x,z)}{\partial x}$ can be evaluated using the formula

$$\int \frac{dz'}{\sqrt{(x - x')^2 - B(z - z')^2}} = \frac{1}{B} \arcsin \frac{B(z - z')}{x - x'} + C \tag{7}$$

and

$$\frac{\partial}{\partial x}\int_{f(x)}^{g(x)} \arcsin\frac{ax'+b}{x-x'}dx' = \varphi$$

with

$$\begin{aligned}\varphi &= \left(1-\frac{df(x)}{dx}\right)\arcsin\frac{af(x)+b}{x-f(x)} - \left(1-\frac{dg(x)}{dx}\right)\arcsin\frac{ag(x)+b}{x-g(x)} \\ &+\frac{a}{\sqrt{a^2-1}}\left(\arcsin\frac{(a^2-1)g(x)+ab+x}{ax+b} - \arcsin\frac{(a^2-1)f(x)+ab+x}{ax+b}\right)\end{aligned} \quad (8)$$

After some algebraic operation, it can be shown that the expression (6) for C_p reduces to (4) with

$$\Gamma_1(m_1,\eta) = \frac{1}{2}+\frac{1}{\pi}\arcsin\frac{-m_1\eta+1}{-m_1+\eta} \quad (9)$$

and

$$\Gamma_2(m_2,\eta) = \frac{1}{2}-\frac{1}{\pi}\arcsin\frac{m_2\eta+1}{m_2+\eta} \quad (10)$$

Consider a symmetrical delta wing with $\chi = \chi_1$ on both leading edges; we have, according to Puckett [3]

$$C_p^{(3d)}(\chi_1,\chi_1) = \frac{4\alpha m_1}{\pi B\sqrt{m_1^2-1}}\arccos\sqrt{\frac{1-\eta^2}{m_1^2-\eta^2}} \quad (11)$$

where $m_1 = B/\tan\chi_1$.

Now consider a symmetrical delta wing with $\chi = \chi_2$ on both leading edges; we have, according to Puckett [3]

$$C_p^{(3d)}(\chi_2,\chi_2) = \frac{4\alpha m_2}{\pi B\sqrt{m_2^2-1}}\arccos\sqrt{\frac{1-\eta^2}{m_2^2-\eta^2}} \quad (12)$$

where $m_2 = B/\tan\chi_2$.

One would expect that $C_p^{(3d)}(\chi_2,\chi_2)$ can be obtained by adding the pressure coefficient for a symmetrical delta wing with $\chi = \chi_1$ and half of the difference $C_p^{(3d)}(\chi_2,\chi_2) - C_p^{(3d)}(\chi_1,\chi_1)$. This would give

$$\Gamma_1(m_1,\eta) = \frac{1}{\pi}\arccos\sqrt{\frac{1-\eta^2}{m_1^2-\eta^2}}, \Gamma_2(m_2,\eta) = \frac{1}{\pi}\arccos\sqrt{\frac{1-\eta^2}{m_2^2-\eta^2}} \quad (13)$$

The Formula (4) with $\Gamma_1(m_1,\eta)$ and $\Gamma_2(m_2,\eta)$ given by (13) reduces to the exact solution of Puckett [3] for a symmetric delta wing

$$C_p^{(3d)} = \frac{4\alpha m}{\pi B\sqrt{m^2-1}}\arccos\sqrt{\frac{1-\eta^2}{m^2-\eta^2}} \quad (14)$$

However, it can be shown that, at the 2D/3D edges ($\eta = \pm 1$), (13) does not bridge continuously with the 2D solutions (1) and (2).

To ensure continuity at the edges, a simple way is to modify (13) as

$$\Gamma_1(m_1,\eta) = \frac{1+\eta}{2\pi}\arccos\sqrt{\frac{1-\eta^2}{m_1^2-\eta^2}}, \Gamma_2(m_2,\eta) = \frac{1-\eta}{2\pi}\arccos\sqrt{\frac{1-\eta^2}{m_2^2-\eta^2}}. \quad (15)$$

3. Nonlinear Approximation by Geometric Transformation

In the nonlinear extension, we consider inviscid flow and focus on the lower surface with an attached shock wave.

3.1. Geometrical Relations

In the nonlinear case, the shock wave depends not only on the upstream Mach number but also on the angle of attack and the leading edge sweep angle. There are two equivalent ways to define the angle of attack and the sweep angle, as shown in Figures 2 and 3.

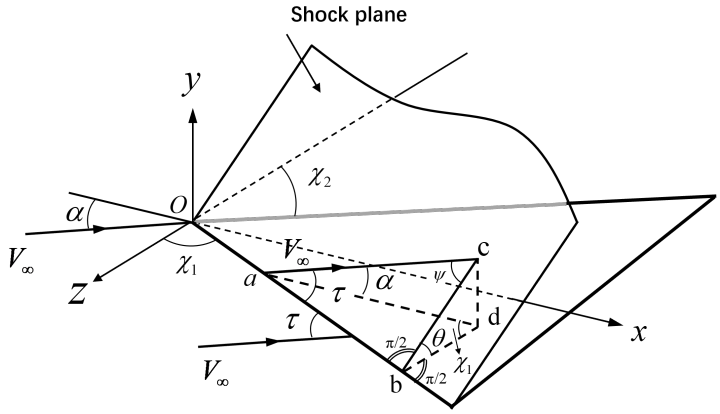


Figure 2. Schematic display of a delta wing at high angle of attack (following Babaev [7]). The coordinate system is defined with x along the chordwise direction, z along the spanwise direction, and y normal to the wing surface.

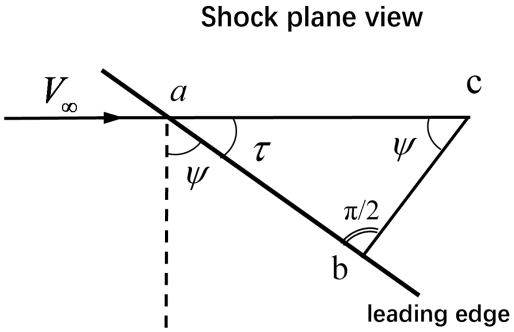


Figure 3. Top view from the top of the shock surface.

The configuration shown in Figure 2 was adopted by some authors, like Babaev [7] and Hui [11]. Here, the free stream velocity passing through the apex (o) lies on the same plane as the x-axis. The y-axis is perpendicular to the wing, and the z-axis is along the span. The wing is on the plane with $y = 0$. The angle of attack α is the angle between the free stream and the x-axis. The sweep is defined as the sweep in the wing surface, i.e., in the $x - z$ plane; thus, the sweep angle χ is defined as the angle between the leading edge and the spanwise axis (z).

In the present case, the left leading edge sweep angle $\chi = \chi_1$ is different from the right leading edge sweep angle $\chi = \chi_2$. Now consider the left leading edge.

Emanuel [20] and Domel [21] considered the shock wave produced by an infinite span sweep wing. The sweep angle ψ is defined as the sweep in the shock plane, as shown in Figure 3, so

$$\sin\psi = \cos\alpha \sin\chi \tag{16}$$

and the angle of attack θ is defined in the plane normal to the leading edge, so

$$\tan\theta = \frac{\tan\alpha}{\cos\chi}, \tag{17}$$

according to Babaev [7] and Hui [11].

The angle between the free stream velocity and the leading edge is denoted as τ. According to Hui [11],

$$\cos\tau = \cos\alpha\sin\chi.$$

3.2. Shock Solution in the Two-Dimensional or Uniform Region

Numerous authors have given the expressions for shock solutions accounting for the swept angle effect of the leading edge (e.g., Babaev [7]; Akinrelere [10]; Hui [11]; Emanuel [20]; Threadgill & Little [22]). As noted by Hui [11], the flow field on the lower surface of a delta wing consists of uniform flow regions near the leading edges, where the cross flow is supersonic, and a nonuniform flow region near the central part. Now we provide the shock expressions for the uniform region.

The Domel's 3D theta–beta–Mach-sweep ($\theta-\beta-Ma-\psi$) shock relations are written in a form very similar to the two-dimensional counterpart and easy to use here. As commented by Threadgill & Little [22], Domel [21]'s theta–beta–Mach-sweep shock relations have been derived for an infinite-span swept oblique inviscid shock. However, the uniform flow region of the delta wings can be described by the infinite-span swept oblique shock relations.

Note that the sweep angle ψ and the angle of attack θ in Domel's definitions are related to those in the definitions of Babaev [7] and Hui [11] by (16) and (17).

Domel discovered the existence of an effective 2D plane that can be obtained by rotation of his y plane (this y is the axis normal to the shock surface) by a tilt angle (ϕ), and on this effective plane, he introduced the effective deflection angle θe and the effective shock angle β_e. First, the effective shock angle β_e is solved by

$$\tan\theta = \frac{1}{\sin\beta_e}\frac{\left(Ma_\infty^2\sin^2\beta_e-1\right)\sqrt{1-\sin^2\beta_e\left(1+\tan^2\psi\right)}}{\frac{\gamma+1}{2}Ma_\infty^2-\left(Ma_\infty^2\sin^2\beta_e-1\right)\left(1+\tan^2\psi\right)} \tag{18}$$

and then the effective deflection angle θe is solved by

$$\tan\theta_e = \frac{1}{\sin\beta_e}\frac{\left(Ma_\infty^2\sin^2\beta_e-1\right)\sqrt{1-\sin^2\beta_e}}{\frac{\gamma+1}{2}Ma_\infty^2-\left(Ma_\infty^2\sin^2\beta_e-1\right)} \tag{19}$$

Once β_e is obtained by (18), and θ_e is obtained by (19), the Mach number M, the pressure p, and the density ρ downstream of the shock wave are computed by

$$Ma = \frac{1}{\sin(\beta_e-\theta_e)}\sqrt{\frac{Ma_\infty^2\sin^2\beta_e+\frac{2}{\gamma-1}}{\frac{2\gamma}{\gamma-1}Ma_\infty^2\sin^2\beta_e-1}} \tag{20}$$

$$p = p_\infty\left(1+\frac{2\gamma}{\gamma+1}\left(Ma_\infty^2\sin^2\beta_e-1\right)\right) \tag{21}$$

$$\rho = \rho_\infty\frac{(\gamma+1)Ma_\infty^2\sin^2\beta_e}{(\gamma-1)Ma_\infty^2\sin^2\beta_e+2} \tag{22}$$

Using (21), the pressure coefficient is

$$C_p = \frac{4}{\gamma+1}(\sin^2\beta_e - \frac{1}{Ma_\infty^2}) \tag{23}$$

For the two-dimensional region close to the left leading edge, $\chi = \chi_1$ and (18)–(21) are used to obtain Ma and C_p, which are set to be Ma_1 and $C_{p,1}^{(2d)}$.

For the two-dimensional region close to the right leading edge, $\chi = \chi_2$ and (18)–(21) are used to obtain Ma and C_p, which are set to be Ma_2 and $C_{p,2}^{(2d)}$.

3.3. Geometric Transformation

To extend the linear expression to nonlinear cases directly, we need a geometrical transformation. Bai & Wu [18] proposed such a method when extending the Heaslet & Lomax [19] linear solution for starting flow at a small angle of attack to a nonlinear case at a large angle of attack. This geometric transformation is used to make the linear expression in a form that is invariant to frame rotation and nonlinear extension.

To write the geometrical transformation in a more convenient way, the positions of the left boundary and right boundaries of the wing are denoted as

$$z_1^{(l)} = \frac{x}{\tan\chi_1},\ z_2^{(l)} = -\frac{x}{\tan\chi_2}, \tag{24}$$

and the positions of the left boundary and right boundaries of the Mach cone from the apex (O) are denoted as

$$z_1^{(m)} = x\tan\mu_\infty,\ z_2^{(m)} = -x\tan\mu_\infty \tag{25}$$

Now, we want to express the parameters m_1, m_2, and η involved in the pressure expression (4) in terms of the boundaries defined by (24) and (25). Using $m_1 = \frac{1}{\tan\chi_1\tan\mu_\infty}$ and $m_2 = \frac{1}{\tan\chi_2\tan\mu_\infty}$, and using (24) and (25), we get

$$m_1 = \frac{z_1^{(l)}}{z_1^{(m)}} \tag{26}$$

and

$$m_2 = \frac{z_2^{(l)}}{z_2^{(m)}} \tag{27}$$

By (3), we have $\eta = \frac{z}{x\tan\mu_\infty}$, and using (24) and (25), we get

$$\eta = \frac{z - \widetilde{z}^{(m)}}{\frac{1}{2}\Delta z^{(m)}} \tag{28}$$

where

$$\widetilde{z}^{(m)} = \frac{z_1^{(m)} + z_2^{(m)}}{2} = \frac{x\tan\mu_1 - x\tan\mu_2}{2} \tag{29}$$

is the average of the two boundaries $z_1^{(m)}$ and $z_2^{(m)}$ and

$$\Delta z^{(m)} = z_1^{(m)} - z_2^{(m)}$$

is the width of the three-dimensional region.

3.4. Nonlinear Solution for the Three-Dimensional Region

In the nonlinear case, the left and right boundaries of the wing are still given by (24); the left and right boundaries of the Mach cone, or the edges between the two-dimensional regions and the three-dimensional region, are no longer given by (25), but are given by

$$z_1^{(m)} = x \tan \mu_1,\ z_2^{(m)} = -x \tan \mu_2 \tag{30}$$

where $\mu_1 = \arcsin \frac{1}{Ma_1}$ and $\mu_2 = \arcsin \frac{1}{Ma_2}$, Ma_1 are the Mach numbers in the left two-dimensional flow region downstream of the shock wave, and Ma_2 is the Mach number in the right two-dimensional flow region downstream of the shock wave.

The parameters m_1, m_2, and η are still determined by the expressions (26), (27), and (28), with $z_1^{(m)}$ and $z_2^{(m)}$ determined by (30). The pressure coefficients $C_{p,1}^{(2d)}$ and $C_{p,2}^{(2d)}$, along with Ma_1 and Ma_2, are replaced by the nonlinear solution given in Section 3.2.

The nonlinear pressure coefficient in the 3D region is postulated to have the same form as (4), i.e.,

$$C_p^{(3d)} = C_{p,1}^{(2d)} \Gamma_1(m_1, \eta) + C_{p,2}^{(2d)} \Gamma_2(m_2, \eta) \tag{31}$$

where $\Gamma_1(m_1, \eta)$ is given by (9), $\Gamma_2(m_2, \eta)$ is given by (10), $C_{p,1}^{(2d)}$ and $C_{p,2}^{(2d)}$ are given by the 2D shock solution in Section 3.2, m_1 is given by (26), m_2 is given by (27), and η is given by (28).

4. Comparison with Exact Method

4.1. Symmetric Delta Wing

Babaev [7], Kutler & Lomax [23], Bluford [16], Woods & McIntosh [9], Roe [13], and Woods [17] provided various cases that can be used to check the approximate yet very simple method provided above.

Table 1 displays β_e computed by (18), θ_e by (19), Ma by (20), and C_p by (23) for several cases. Consider, for instance, case 1; Babaev [7] and Hui [11] give $C_p = 0.26$, which is the same as given by Domel's shock expressions.

Table 1. Shock solution for four cases.

Case	Ma_∞	χ, α	ψ, θ	β_e, θ_e (Domel)	Ma	C_p (Domel)
1	4.0	50°, 15°	47.73°, 15.66°	27.85°, 15.77°	2.874	0.260
2	5.08	50°, 14°	48.01°, 14.55°	23.47°, 14.34°	3.613	0.200
3	4	50°, 16°	47.42°, 16.79°	29.01°, 16.87°	2.795	0.288
4	6	50°, 21°	45.65°, 22.65°	30.03°, 21.51°	3.207	0.371

We check whether the Formula (30) correctly predicts the boundaries between the two-dimensional regions and the three-dimensional region for the symmetric case, as shown in Table 1. In the symmetric case, we consider just the right boundary defined by

$$\varphi = \frac{z_1^{(m)}}{z_1^{(l)}} = \tan \mu \tan \chi \tag{32}$$

where $\mu = \arcsin \frac{1}{Ma}$, with Ma given by (20). The value φ^* is from Babaev [7] for case 1, Woods & McIntosh [9] for cases 2 and 3, from Babaev [7] (see also Roe [13]) for case 3, and from Babaev [7] and Squire [24] for case 4 ($\varphi^* \approx 0.48$ is from Babaev [7] and 0.36 is from Squire [24]). The relative difference $\frac{|\varphi^* - \varphi|}{\varphi^*}$ is also shown in Table 2. Thus, there is some discrepancy between φ predicted by (32) and provided by various previous works.

Table 2. Boundaries between 2D and 3D regions for four cases shown in Table 1.

Case	Ma_∞, χ, α	Ma	φ	φ^*	$\frac{\lvert\varphi^*-\varphi\rvert}{\varphi^*}$
1	$4.0, 50°, 15°$	2.874	0.442	≈0.47	5.96%
2	$5.08, 50°, 14°$	3.613	0.343	≈0.32	7.19%
3	$4, 50°, 16°$	2.795	0.458	≈0.55	16.73%
4	$6, 50°, 21°$	3.207	0.391	≈0.36,0.48	8.61%, 19.05%

Now we check whether the Formula (31) can predict the previous results for the test cases shown in Table 1. In the symmetric case, the minimal value of C_p is given by

$$C_{p,\min} = \left(\frac{2}{\pi}\arccos\frac{1}{m}\right)C_p^{(2d)}$$

where $C_p^{(2d)}$ is given by (23), and $m = \frac{1}{\tan\chi\tan\mu}$.

The results are shown in Table 3, where $C^*_{p,\min}$ is from Babaev [7] for case 1, Woods & McIntosh [9] for case 2, from Babaev [7] (see also Roe [13]) for case 3, and from Babaev [7] and Squire [24] for case 4 ($C^*_{p,\min} \approx 0.30$ is from Babaev [7] and 0.31 is from Squire [24]). The relative difference $\frac{\lvert C^*_{p,\min}-C_{p,\min}\rvert}{C^*_{p,\min}}$ is also shown in Table 1. Thus, the very simple and easy to use formula $C_{p,\min} = \left(\frac{2}{\pi}\arccos\frac{1}{m}\right)C_p^{(2d)}$ can predict the minimum pressure coefficient within a difference of at most 11% compared to very complex and accurate results.

Table 3. Minimum pressure coefficients for four cases shown in Table 1.

Case	M_∞, χ, α	$C_{p,\min}$	$C^*_{p,\min}$	$\frac{\lvert C^*_{p,\min}-C_{p,\min}\rvert}{C^*_{p,\min}}$
1	$4.0, 50°, 15°$	0.184	≈0.19	3.16%
2	$5.08, 50°, 14°$	0.155	≈0.17	8.82%
3	$4, 50°, 16°$	0.201	≈0.20	0.50%
4	$6, 50°, 21°$	0.276	≈0.30,0.31	8.00%, 10.97%

4.2. Yawed Delta Wing

Hui [12] extended his method for symmetric delta wings [11] to the case with a yawed delta wing. He provided results that appear to match the present asymmetric delta wings.

For $Ma_\infty = 4$ and $\alpha = 15°$, Hui [12] considered yawed delta wings that correspond to $\chi_1 = 10°$ and $\chi_2 = 55°$. For $Ma_\infty = 10$ and $\alpha = 10°$, he considered yawed delta wings that correspond to $\chi_1 = 30°$ and $\chi_2 = 75°$. He showed the pressure distribition in their Figure 5 and 6 (we have checked that the conditions marked in their Figure 5 and 6 should be exchanged).

For comparison, we use Domel's expression for $C_{p,1}^{(2d)}$ and $C_{p,2}^{(2d)}$ and the Formula (31) for $C_{p,\min}$. The comparison is displayed in Table 4, where $C_{p,1}^{*(2d)}$, $C_{p,2}^{*(2d)}$ and $C^*_{p,\min}$ are from Figures 5 and 6 of Hui [12]. Here, $C^{(a)}_{p,\min}$ is obtained from (31) with $\Gamma_i(m_i,\eta)$ given by the expression (15) and $C^{(b)}_{p,\min}$ is obtained from (31) with $\Gamma_i(m_i,\eta)$ given by Expressions (9) and (10).

Table 4. Comparison with the results of Hui [12].

Case	Ma_∞, α	χ_1, χ_2	$C_{p1}^{(2d)}$, $C_{p,2}^{(2d)}$	$C_{p,1}^{*(2d)}, C_{p,2}^{*(2d)}$	$C^{(a)}_{p,\min}$	$C^{(b)}_{p,\min}$	$C^*_{p,\min}$
1	$4, 15°$	$10°, 55°$	0.241, 0.276	0.241, 0.278	0.203	0.197	≈0.215
2	$10, 10°$	$30°, 75°$	0.0869, 0.106	0.0868, 0.107	0.072	0.071	≈0.076

The pressure distribution of Hui [12] indicates that the minimum $C_{p,\min}$ occurs at $z \to 0$ or $\eta \to 0$. Figure 4 shows the pressure distribution predicted by (31) with $\Gamma_i(m_i, \eta)$ given by Expression (15). We see that the minimum $C_{p,\min}$ occurs not at $z \to 0$ or $\eta \to 0$. Figure 5 shows the pressure distribution predicted by (31) with $\Gamma_i(m_i, \eta)$ given by Expressions (9) and (10). We see that the minimum $C_{p,\min}$ occurs at $z \to 0$ or $\eta \to 0$. Overall, the pressure distribution predicted by (31) with $\Gamma_i(m_i, \eta)$ given by Expressions (9) and (10) produces well the results of Hui [12] better than Expression (15).

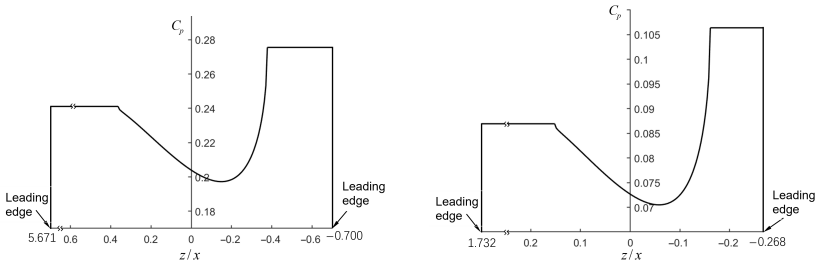


Figure 4. Pressure distribution for the two cases of Hui [11], with $\Gamma_i(m_i, \eta)$ given by (15). (**a**) $Ma_\infty = 4$, $\alpha = 15^\circ$, $\chi_1 = 10^\circ$ and $\chi_2 = 55^\circ$. (**b**) $Ma_\infty = 10$, $\alpha = 10^\circ$, $\chi_1 = 30^\circ$ and $\chi_2 = 75^\circ$.

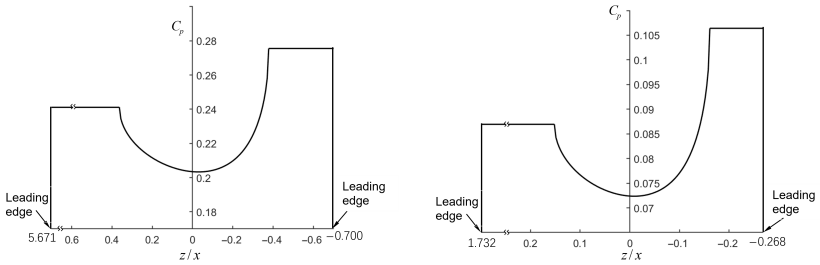


Figure 5. Pressure distribution for the two cases of Hui [11], with $\Gamma_i(m_i, \eta)$ given by Expressions (9) and (10). (**a**) $Ma_\infty = 4$, $\alpha = 15^\circ$, $\chi_1 = 10^\circ$ and $\chi_2 = 55^\circ$. (**b**) $Ma_\infty = 10$, $\alpha = 10^\circ$, $\chi_1 = 30^\circ$ and $\chi_2 = 75^\circ$.

It is interesting to note that, despite the delta wing being highly asymmetric, the centerline of the Mach cone (or position of the minimal value $C_{p,\min}$) coincides almost exactly with the axis $z = 0$ in both Hui [12]'s work and in the present model with $\Gamma_i(m_i, \eta)$ given by Expressions (9) and (10).

To consider more quantitative information about asymmetry, we consider $Ma_\infty = 4$, $\alpha = 15^\circ$ and $\chi_1 = 50^\circ$ for various χ_2. Using Domel's method, we get $C_{p,1}^{(2d)} = 0.260$ and $Ma_1 = 2.874$ (see Table 1). The asymmetry of the position of $C_{p,\min}$ can be measured with

$$\omega = \frac{\tilde{z}^{(m)}}{z_2^{(l)} - z_1^{(l)}} = \frac{1}{2} \frac{\tan \mu_1 - \tan \mu_2}{\frac{1}{\tan \chi_1} + \frac{1}{\tan \chi_2}} \tag{33}$$

where $\tilde{z}^{(m)}$ is the middle of the three-dimensional region defined by (29). In the symmetrical case, $\omega = 0$, so the magnitude of ω characterizes the asymmetry of the three-dimensional region.

Table 5 displays Ma_2, m_1,m_2, $C_{p,2}^{(2d)}$, ω and $C_{p,\min}$ for several choices χ_2, including the symmetric case $\chi_2 = \chi_1 = 50^\circ$. The parameters m_1 and m_2 are computed by (26) and (27), with $z_1^{(m)}$ and $z_2^{(m)}$ determined by (30), i.e.,

$$m_1 = \frac{z_1^{(l)}}{z_1^{(m)}} = \frac{1}{\tan \chi_1 \tan \mu_1}, \; m_2 = \frac{z_2^{(l)}}{z_2^{(m)}} = \frac{1}{\tan \chi_2 \tan \mu_2}$$

The parameter ω is computed by (33), $C_{p,2}^{(2d)}$ is computed with the Domel's Formula (23) for $\chi = \chi_2$, and $C_{p,\min}$ is computed by (31) with $\Gamma_1(m_1, \eta)$ given by (9) and $\Gamma_2(m_2, \eta)$ given by (10).

Table 5. Typical flow parameters for various sweep angles on the right leading edge.

Case	χ_2	M_2	m_1, m_2	$C_{p,2}^{(2d)}$	ω	$C_{p,\min}$
1	50°	2.8736	2.2606, 2.2606	0.2597	0.0000	0.1840
2	52°	2.8605	2.2606, 2.0939	0.2643	−0.0006	0.1822
3	54°	2.8418	2.2606, 1.9326	0.2709	−0.0015	0.1805
4	56°	2.8117	2.2606, 1.7725	0.2817	−0.0031	0.1791
5	58°	2.7410	2.2606, 1.5947	0.3077	−0.0070	0.1795

We see that the asymmetry parameter ω is negative, meaning that the middle line of the three-dimensional region is on the side of the larger sweep angle. The minimum pressure coefficient $C_{p,\min}$ decreases with increasing χ_2. In all cases, the magnitude of ω is very small, showing that the asymmetry of the delta wings does not significantly change in the middle of the three-dimensional region.

5. Lift or Normal Coefficient for Asymmetric Delta Wings

The lift is normal to the incoming flow direction, so the lift coefficient $C_L = C_N \cos\alpha$, where C_N is the normal force coefficient. Here, we show that the normal force coefficient due to the pressure of the lower surface of an asymmetric delta wing at high angles of attack can be expressed as a weighted average of the pressure coefficients in the two uniform flow regions near the left and right leading edges.

The schematic display Figure 1 for the linear case is replaced by Figure 6 in the nonlinear case. In the latter case, the Mach waves OC and OD are not symmetric with respect to the x-axis. Moreover, for $\chi_2 > \chi_1$, it can be shown that $\mu_2 < \mu_1$, at least for the conditions shown in Table 4.

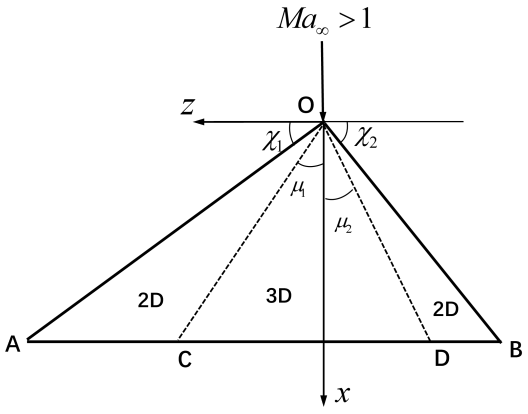


Figure 6. Schematic display of a delta wing in the nonlinear case.

The normal force coefficient is obtained by integrating the pressure over the wing surface:

$$C_N = \frac{1}{S}\left(C_{p,1}^{(2d)} S_1 + C_{p,2}^{(2d)} S_2 + I^{(3d)}\right) \tag{34}$$

where $S = \frac{h^2}{2}(\cot\chi_1 + \cot\chi_2)$ is the reference area of the delta wings, $S_1 = \frac{h^2}{2}(\cot\chi_1 - \tan\mu_1)$ is the area of the left two-dimensional flow region (h is the height of the delta wing),

$S_2 = \frac{h^2}{2}(\cot\chi_2 - \tan\mu_2)$ is the area of the right two-dimensional flow region, and $I^{(3d)} = \int_{S_{OCD}} C_p^{(3d)} dxdz$. With the expression (31), we get $\frac{z-\tilde{z}^{(m)}}{\frac{1}{2}\Delta z^{(m)}}$

$$I^{(3d)} = V_1 C_{p,1}^{(2d)} + V_2 C_{p,2}^{(2d)} \tag{35}$$

where

$$V_1 = \int_{S_{OCD}} \Gamma_1(m_1,\eta)dxdz, V_2 = \int_{S_{OCD}} \Gamma_2(m_2,\eta)dxdz$$

where $\Gamma_1(m_1,\eta)$ and $\Gamma_2(m_2,\eta)$ are given by (9) and (10), and η is defined by (28).

Define

$$J_1(m_1) = \frac{B}{h^2}\int_0^h \int_{z_2^{(m)}}^{z_1^{(m)}} \Gamma_1(m_1,\eta)dzdx,\ J_2(m_2) = \frac{B}{h^2}\int_0^h \int_{z_2^{(m)}}^{z_1^{(m)}} \Gamma_2(m_2,\eta)dzdx, \tag{36}$$

where $z_2^{(m)}$ and $z_1^{(m)}$ are defined by (30); then, $V_1 = \frac{h^2}{B}J_1(m_1)$ and $V_2 = \frac{h^2}{B}J_2(m_2)$, and using (35), we get from (34) the following compact form for C_N

$$C_N = W_1\, C_{p,1}^{(2d)} + W_2\, C_{p,2}^{(2d)} \tag{37}$$

where

$$W_1 = \frac{\cot\chi_1 - \tan\mu_1}{\cot\chi_1 + \cot\chi_2} + \frac{J_1(m_1)}{B}\frac{2}{\cot\chi_1 + \cot\chi_2} \tag{38}$$

and

$$W_2 = \frac{\cot\chi_2 - \tan\mu_2}{\cot\chi_1 + \cot\chi_2} + \frac{J_2(m_1)}{B}\frac{2}{\cot\chi_1 + \cot\chi_2} \tag{39}$$

Note that $C_{p,i}^{(2d)}$ $(i = 1, 2)$ are the pressure coefficients in the two-dimensional uniform flow regions (given by shock relations in Section 3.2), and the weights W_i are functions of $m_i, \mu_i = \arcsin\frac{1}{M_i}$ and χ_i.

For a symmetric delta wings with $\chi_1 = \chi_2 = \chi$, we have $C_{p,1}^{(2d)} = C_{p,2}^{(2d)} = C_p^{(2d)}$, $\mu_1 = \mu_2 = \mu$, $m_1 = m_2 = m$, and Equation (37) can be shown to give

$$C_N = C_p^{(2d)} \cdot \frac{\sqrt{m^2-1}}{m}. \tag{40}$$

In the linear limit (small angle of attack α and small disturbances), $C_p^{(2d)} = 2\alpha m/(B\sqrt{m^2-1})$, where $B = \sqrt{Ma_\infty^2 - 1}$. Substituting this into Equation (40) yields

$$C_N = \frac{2\alpha}{B} = \frac{2\alpha}{\sqrt{Ma_\infty^2 - 1}}. \tag{41}$$

This is exactly one-half of the lift coefficient given by Puckett [3] for a symmetric delta wing (which includes both upper and lower surfaces). See also Stewart [2] for the lift when the leading edge is subsonic. Puckett's result for the entire wing is $C_L = 4\alpha/\sqrt{Ma^2-1}$; thus, the present formula correctly recovers the lower-surface contribution in the linear symmetric limit.

6. Conclusions

This paper presents an approximate analytical method based on geometric transformation for predicting the pressure distribution on asymmetric delta wings with attached shock waves at high angles of attack. By reformulating the linear solution into a geometrically invariant form and replacing the pressure coefficients in the two-dimensional regions with those given by shock relations, a simple algebraic-type formula with clear physical meaning

is derived. The core idea is to use geometric transformation as a bridge connecting the nonlinear flow problem to known linear solutions, analogous to the approach used in studies of supersonic starting flow at high incidence. The normal force coefficient is also obtained. The method is validated against existing reference solutions for both symmetric and asymmetric (yawed) delta wings.

The main contribution of this study lies in providing a physically transparent pathway for analyzing asymmetric delta wings under complex conditions. It avoids the substantial computational effort typically required by sophisticated perturbation theories or numerical simulations. The resulting formulas are simple and compact, making them suitable for further extensions that account for viscous effects.

Currently, the method primarily addresses the lower surface. Extension to the upper surface—which involves more complex three-dimensional expansion waves and possible inboard shocks—requires further treatment of intricate wave interactions (a conceptual pathway is outlined in Appendix A, though it remains unvalidated).

Author Contributions: Conceptualization, Z.-N.W. and X.-Y.W.; methodology, X.-Y.W.; validation, X.-Y.W.; formal analysis, X.-Y.W.; investigation, X.-Y.W.; writing—original draft preparation, Z.-N.W.; writing—review and editing, X.-Y.W., J.P.; visualization, X.-Y.W.; supervision, J.P.; project administration, Z.-N.W.; funding acquisition, Z.-N.W. All authors have read and agreed to the published version of the manuscript.

Funding: This research was funded by the National Key Project, grant number GJXM92579.

Data Availability Statement: The original contributions presented in the study are included in the article, further inquiries can be directed to the corresponding author.

Acknowledgments: The authors are grateful for the comments that helped to improve the paper. This work was supported partly by the National Key Project (grant no. GJXM92579).

Conflicts of Interest: The authors declare no conflicts of interest.

Appendix A. Possible Extension for the Upper Surface

Despite the linear solution sharing the same form on both the lower and upper surfaces, the nonlinear solution on the upper surface is far more complex than on the lower surface. Babaev [15] pointed out that apart from a three-dimensional Prandtl–Meyer expansion wave, there is also an inboard shock. The reason is that the streams from two halves of the wing, having velocity components equal in magnitude but opposite in direction, tend to meet on the plane of symmetry of the wing, and a shockwave must arise, on crossing which and behind which the stream changes to a direction parallel to the root chord. Even for the Prandtl–Meyer expansion wave, a numerical integration of the characteristic equation is required to find the flow properties in the uniform flow region. Fowell [14] studied a plane delta wing with supersonic leading edges. An exact analysis based upon the equations for inviscid flow with constant stagnation enthalpy showed the existence of two cases in the solution of the flow over the expansion surface; below a critical angle of attack, a continuous solution can exist, while above this angle, the solution must be discontinuous.

Using the three-dimensional method of characteristics, Beeman & Powers [25] identified four regions of flow on the upper surface. Kutler & Lomax [23] used computational fluid dynamics to study high-angle-of-attack flow around a delta wing, and noted that Babaev fails to predict the correct values of the flow quantities in the region of uniform flow adjacent to the wing surface and between the inboard shock wave and the wing leading edge.

Bannink & Nebbeling [26] experimentally studied the flow around a delta wing, and arrived at the conclusion that the inviscid flow field at the expansion side of the delta wings

appears to be conical and suggested that the inboard shock wave ends with zero strength at the point where the conical sonic line starts.

Neglecting the effect of the inboard shock, the present method can be extended to the upper surface in the following way.

First, determine the Mach number Ma and pressure coefficients $C_p^{(2d)}$ in the two-dimensional uniform region using the Prandtl–Meyer solution of Vahrenkamp [27] with sweep (χ), angle of attack (α), and upstream Mach number (Ma_∞) in his M.S. thesis (Section 10.3 of Emanuel [20]). This is carried out for the two-dimensional region along each side of the delta wings, with different sweep angles χ_1 and χ_2.

Then, compute the boundaries of the three-dimensional regions by (30), where $\mu_1 = \arcsin \frac{1}{Ma_1}$ and $\mu_2 = \arcsin \frac{1}{Ma_2}$, Ma_1 are the Mach numbers in the left two-dimensional flow region downstream of the Prandtl–Meyer wave, and Ma_2 is the Mach number in the right two-dimensional flow region downstream of the Prandtl–Meyer wave.

The pressure coefficient in the three-dimensional region is computed by (31), in the same way as for the lower surface, except that the pressure coefficients are given by Vahrenkamp's expression.

Finally, the normal force coefficient due to the upper surface is computed by (37), in the same way as for the lower surface, except that μ_1, μ_2, and the pressure coefficients are based on Vahrenkamp's expression.

References

1. Jones, R.T. *Properties of Low-Aspect-Ratio Pointed Wings at Speeds Below and Above the Speed of Sound*; NACA Report 835; NASA: Washington, DC, USA, 1946.
2. Stewart, H.J. The lift of a delta wing at supersonic speeds. *Q. Appl. Math.* **1946**, *4*, 246–254. [CrossRef]
3. Puckett, A.E. Supersonic Wave Drag of Thin Airfoils. *J. Aeronaut. Sci.* **1946**, *13*, 475–484. [CrossRef]
4. Ackeret, J. Air Forces on Airfoils Moving Faster than Sound. In *Zeitschrift fur Flugtechnik und Motorluftschiffahrt*; NASA: Washington, DC, USA, 1925; pp. 72–74. English Trans. as NACA Technical Memorandum No. 317, 1935.
5. Goodman, T.R. The lift distribution on conical and non-conical flow regions of thin finite wings in a supersonic stream. *J. Aeronaut. Sci.* **1949**, *16*, 365–374. [CrossRef]
6. Malvestuto, F.S., Jr.; Margolis, K.; Reiner, H.S. *Theoretical Lift and Damping in Roll at Supersonic Speeds of Thin Sweptback Tapered Wings with Streamwise Tips, Subsonic Leading Edges, and Supersonic Trailing Edges*; NACA Report 970; NASA: Washington, DC, USA, 1950.
7. Babaev, D.A. Numerical solution of the problem of supersonic flow past the lower surface of a delta wing. *AIAA J.* **1963**, *1*, 2224–2231. [CrossRef]
8. Messiter, A.F. Lift of slender delta wings according to Newtonian theory. *AIAA J.* **1963**, *1*, 794–802. [CrossRef]
9. Woods, B.A.; McIntosh, C.B.G. Hypersonic flow with attached shock waves over plane delta wings. *J. Fluid Mech.* **1977**, *79*, 361–377. [CrossRef]
10. Akinrelere, E.A. The calculation of inviscid hypersonic flow past the lower surface of a delta wing. *J. Fluid Mech.* **1970**, *44*, 113–127. [CrossRef]
11. Hui, W.H. Supersonic and hypersonic flow with attached shock waves over delta wings. *Proc. R. Soc. Lond. Ser. A* **1971**, *325*, 251–268. [CrossRef]
12. Hui, W.H. Effect of yaw on supersonic and hypersonic flow over delta wings. *Aeronaut. J.* **1973**, *77*, 299–301. [CrossRef]
13. Roe, P.L. *A Result Concerning the Supersonic Flow Below a Plane Delta Wing (CP No. 1228)*; Her Majesty's Stationery Office: London, UK, 1972.
14. Fowell, L.R. Exact and Approximate Solutions for the Supersonic Delta Wing. *J. Aeronaut. Sci.* **1956**, *23*, 709–720. [CrossRef]
15. Babaev, D.A. Numerical solution of the problem of supersonic flow past the upper surface of a delta wing. *Zhur. Vychisli Tel'noi Matematiki i Matematicheskoi Fiziki (J. Comput. Math. Math. Phys.)* **1962**, *2*, 278–289.
16. Bluford, G.S. Numerical Solution of the Supersonic and Hypersonic Viscous Flow around Thin Delta Wings. *AIAA J.* **1979**, *17*, 942–949. [CrossRef]
17. Wood, R.M. *Supersonic Aerodynamics of Delta Wings*; NASA TP-2771; NASA: Washington, DC, USA, 1988.
18. Bai, C.Y.; Wu, Z.N. Supersonic indicial response with nonlinear corrections by shock and rarefaction waves. *AIAA J.* **2017**, *55*, 884–892. [CrossRef]
19. Heaslet, M.A.; Lomax, H. *Two-Dimensional Unsteady Lift Problems in Supersonic Flight*; Archiveand Image Library TR 945, also NACA TN-1621; NASA: Washington, DC, USA, 1948.

20. Emanuel, G. *Analytical Fluid Dynamics*, 2nd ed.; CRC Press: Boca Raton, FL, USA, 2000.
21. Domel, N.D. General three-dimensional relation for oblique shocks on swept ramps. *AIAA J.* **2016**, *54*, 310–319. [CrossRef]
22. Threadgill, J.A.S.; Little, J.C. An inviscid analysis of swept oblique shock reflections. *J. Fluid Mech.* **2020**, *890*, A22. [CrossRef]
23. Kutler, P.; Lomax, H. Shock-capturing, finite-difference approach to supersonic flows. *J. Spacecr. Rocket.* **1971**, *8*, 1179–1182. [CrossRef]
24. Squire, L.C. Calculated pressure distributions and shock shapes on conical wings with attached shock waves. *Aeronaut. Q.* **1968**, *19*, 31–50. [CrossRef]
25. Beeman, E.; Powers, S. A method for determining the complete flow field around conical wings at supersonic/hypersonic speeds. In Proceedings of the AIAA Fluid and Plasma Dynamics Conference, San Francisco, CA, USA, 16–18 June 1969.
26. Bannink, W.J.; Nebbeling, C. Investigation of the expansion side of a delta wing at supersonic speed. *AIAA J.* **1973**, *11*, 1151–1156. [CrossRef]
27. Vahrenkamp, M. Prandtl–Meyer Flow with Sweep. Master's Thesis, University of Oklahoma, Norman, OK, USA, 1992.

Disclaimer/Publisher's Note: The statements, opinions and data contained in all publications are solely those of the individual author(s) and contributor(s) and not of MDPI and/or the editor(s). MDPI and/or the editor(s) disclaim responsibility for any injury to people or property resulting from any ideas, methods, instructions or products referred to in the content.